INTERNATIONAL JOURNAL FOR NUMERICAL AND ANALYTICAL METHODS IN GEOMECHANICS
Int. J. Numer. Anal. Meth. Geomech. 2010; **34**:733–753
Published online 3 August 2009 in Wiley InterScience (www.interscience.wiley.com). DOI: 10.1002/nag.829

An iterative pressure-stabilized fractional step algorithm in saturated soil dynamics

Xikui Li[1,*,†], Xue Zhang[1], Xianhong Han[1] and D. C. Sheng[2]

[1]*The State Key Laboratory for Structural Analysis of Industrial Equipment, Dalian University of Technology, Dalian 116024, People's Republic of China*
[2]*School of Engineering, University of Newcastle, Callaghan, NSW 2308, Australia*

SUMMARY

This paper presents an iterative, incremental pressure-stabilized fractional step algorithm for coupled hydro-mechanical problems with mixed formulations of the displacement–pressure (**u**–p) model in saturated soil dynamics that allows the use of finite elements with equal low order of interpolation approximation of **u** and p. In comparison with the original fractional step algorithm, the distinct features of the proposed algorithm lie in its enhanced stability owing to the introduction of both an iteration procedure and a finite increment calculus (FIC) process into the algorithm. The introduction of the iterative procedure makes the velocity term satisfy the momentum conservation equation in an implicit sense and allows much larger time step sizes to be used than those limited in existing explicit and semi-implicit versions of the algorithm. The introduction of the FIC process removes the dependence of the stability of the proposed algorithm on the time step size, as a result it allows to using the incremental version of the algorithm and evades the minimum time step size requirement presented in the existing versions of the fractional step algorithm that restricts the application of the algorithm to saturated soil dynamics problems with high frequencies.

Numerical experiments demonstrate the effectiveness and improved performance of the proposed iterative pressure-stabilized fractional step algorithm. Copyright © 2009 John Wiley & Sons, Ltd.

Received 28 February 2009; Revised 28 May 2009; Accepted 5 June 2009

KEY WORDS: saturated soil dynamics; fractional step algorithm; finite increment calculus; undrained conditions; incompressibility

*Correspondence to: Xikui Li, The State Key Laboratory for Structural Analysis of Industrial Equipment, Dalian University of Technology, Dalian 116024, People's Republic of China.
†E-mail: xikuili@dlut.edu.cn

Contract/grant sponsor: National Natural Science Foundation of China; contract/grant numbers: 10672033, 90715011, 10590354
Contract/grant sponsor: National Key Basic Research and Development Program 973 Program; contract/grant number: 2010CB731502

1. INTRODUCTION

The discretization of the $\mathbf{u}$–p model for saturated soils results in the semi-discrete system of mixed type in displacements and pressures. As it is assumed that both water and soil grains are incompressible and the permeability is so low that its value is negligible, the $\mathbf{u}$–p interpolation function spaces have to be chosen to fulfill the Ladyshenskaya–Babuska–Brezzi (abbreviated as LBB) condition [1–3] or the much simpler Zienkiewicz–Taylor patch test [4, 5] to achieve unique solvability and convergence.

Though simple elements with the equal low order of interpolation for $\mathbf{u}$ and p, such as the linear triangle P1P1 or the 4-noded bi-linear quadrilateral Q1Q1 [6], present important advantages in the speed of computation and the convenience of using adaptive remeshing techniques, they cannot be used in situations close to the incompressible undrained limit as severe spurious oscillations can develop in the pressure field.

The restrictions imposed by the LBB condition in the interpolation approximations of $\mathbf{u}$–p variables can be circumvented by using suitable stabilization techniques such as the fractional step method which was initially devised by Chorin [7, 8]. Even though the original purpose of the method presented by Chorin [7, 8] is to allow the use of standard time integration techniques in incompressible fluid dynamics, the method was found to provide the stabilization for the use of finite elements with equal low–order interpolations of velocities and pressures in the following studies by Schneider *et al.* [9], Kawahara and Ohmiya [10], de Sampaio [11] and was justified later by Zienkiewicz *et al.* [12]. The fractional step algorithm (FSA) was then extended to soil mechanics problems by Pastor *et al.* [13–15]. Pastor *et al.* [15] presented a stabilization technique, in which P1P1 elements in combination with adaptive remeshing techniques were applied to obtain limit loads and failure surfaces in boundary value problems.

One serious disadvantage of original FSA proposed in the past is the over severe limitation on the time step size required to ensure stability of the algorithms due to their explicit nature.

Further studies in the numerical stability of the FSA [16] concluded that it can circumvent the restriction imposed by the LBB condition in the time-dependent, incompressible undrained $\mathbf{u}$–p equations only if the non-incremental version of the algorithm, in which all the pressure gradient term is removed from the first step of the algorithm, is used with the time step size larger than a critical value.

However, this minimum time step size requirement may lead to over a large time step being used, resulting in over-diffusive numerical results, on the other hand, will possibly conflict with the maximum time step size limitation required to use for original FSA due to their fully or partially explicit nature as mentioned above.

Moreover, it is widely accepted that the incremental version of the algorithm, in which the pressure gradient at the previous time level leaves in the first step of the algorithm and computes its increment in the second one will generally provide the results with higher accuracy than those obtained by the non-incremental version [16].

To be brief, the original FSA may suffer numerical instability for the following three reasons, i.e. as (1) the time step size is larger than the maximum time step size used or (2) the time step size is smaller than the minimum time step requirement used or (3) the incremental version of the algorithm is used.

To enhance the stability of original FSA relating to the first instability source and to use time step sizes much larger than the maximum time step size limitation, an iterative stabilized fractional step algorithm (IFSA) was introduced to make the velocity term satisfy the momentum conservation

DOI: 10.1002/nag

equation in an implicit sense, and to result in saving the computational effort in a decisive manner [17]. The prominent performance of the IFSA in this aspect has been demonstrated in [17]. It should be stressed that the iterative procedure introduced into the algorithm will less expend computational efficiency, particularly in view of non-linearity of most of the geo-mechanical problems in which an iterative process is essentially required to satisfy the non-linear momentum conservation condition.

However, the second and the third instability sources mentioned above, i.e. the minimum time step size requirement and the exclusion of the incremental version of the algorithm still restrict the application of the algorithm to the analysis of dynamic responses with from medium to high frequencies in soil dynamic problems, in which a time step smaller than the minimum time step size has to be taken, and both accuracy and efficiency of the algorithm, deteriorate respectively.

To evade the latter two instability factors existing in the original FSA and the proposed IFSA, i.e. to further remove the dependence of the stability of the proposed IFSA on the time step size and allow to using the incremental version of the algorithm, an iterative pressure-stabilized fractional step algorithm abbreviated as PS-IFSA is presented in this paper by means of introduction of the finite increment calculus (FIC) process into previously proposed IFSA [17].

The FIC process is one further simple process as compared with the Petrov–Galerkin approximations and many other procedures [18]. It can be considered, in principle, as a general stabilization process to eliminate numerical instabilities stemming from different sources. Nevertheless when initially presented by Oñate [19], it was only particularly applied to reformulate the momentum conservation equation for restraining the instability due to the convection operator in fluid dynamic problems. Whereas the FIC process is introduced into the present work to consistently modify the mass conservation equation in saturated soil dynamics. Hence, the discretized mixed equations of the $\mathbf{u}-p$ model are re-formulated as irreducible and the instability associated with incompressibility stabilization is restrained even eliminated.

It will be demonstrated later in Section 5 of the present paper that the mechanisms of the instability of the existing FSA algorithms due to the latter two sources are related to a stabilization term proportional to the time step size as well as the pressure difference between the two successive time levels as the incremental version of the FSA, i.e. $\gamma=1$ is adopted. The stabilization term will approach to null and spurious oscillations will occur in the resulting pressure field as the time step is taken with a small value violating the minimum time step requirement or/and the simulated problem approaches to a nearly steady state when the incremental version of the algorithm is adopted.

The merit of the introduction of the FIC process into the proposed algorithm is to introduce an additional stabilization term-independent from the time step size used and the pressure difference between the two successive time levels so that the mass conservation equation in the incompressible limit is still effectively stabilized by the additional stabilized term when a time step with a small value violating the minimum time step requirement is taken or/and the incremental version of the algorithm is adopted.

The performance of the proposed PS-IFSA will be further demonstrated in the section of 'Numerical Examples' of this paper. It will be observed that as equal low-order $\mathbf{u}$–p mixed finite elements are used, the proposed PS-IFSA is capable of preserving the pressure stabilization not only to the low-frequency response problems, for which large time step sizes should be used to enhance the computational efficiency, but also to the high-frequency response ones, for which small time step sizes have to be taken to ensure computational accuracy. In addition, the incremental version of the algorithm can be successfully adopted to ensure accuracy and efficiency of the proposed PS-IFSA.

DOI: 10.1002/nag

The paper is structured as follows. In the next section the governing equations of saturated soil dynamics using the $\mathbf{u}$–p model is briefly introduced. Then the pressure-stabilized governing equations are derived in Section 3 as the FIC process is introduced into the $\mathbf{u}$–p model. With an operator split procedure, the proposed iterative PS-IFSA is formulated in Section 4. Then pressure stability analysis will be performed in Section 5. Finally, the advantage of the proposed algorithm due to the introduction of the FIC process in enhancing the stability over existing versions of the FSA is further validated via numerical results given in Section 6.

2. GOVERNING EQUATIONS OF SATURATED SOIL DYNAMICS

Among the different alternative formulations of saturated soil dynamics, we focus on the $\mathbf{u}$–p model, proposed by Zienkiewicz and Shiomi [20], which is valid for most problems of saturated soil dynamics ranging from low to medium and moderate to high-speed phenomena and approximately valid for those with high-frequency responses as the terms relating to pore fluid acceleration are assumed negligible. Governing equations of this model can be summarized in the forms (1) and (2) given below:

The balance of momentum of the mixture

$$\mathbf{S}^{\mathrm{T}}\boldsymbol{\sigma}' - \nabla p + \rho_m \mathbf{b} - \rho_m \frac{\mathrm{d}\mathbf{v}}{\mathrm{d}t} = 0 \tag{1}$$

A combination of the balance of mass and momentum for the interstitial fluid

$$\nabla^{\mathrm{T}}\mathbf{v} - \nabla^{\mathrm{T}}(k\nabla p) + \frac{\dot{p}}{Q^*} = 0 \tag{2}$$

where $\boldsymbol{\sigma}'$ is the effective stress vector [20] defined as

$$\boldsymbol{\sigma}' = \boldsymbol{\sigma} + \mathbf{m}p \tag{3}$$

in which $\boldsymbol{\sigma}$ is the total Cauchy stress vector in the mixture. The operator matrix $\mathbf{S}$, vectors $\boldsymbol{\sigma}'$ and $\mathbf{m}$ in the two-dimensional case take the forms

$$\mathbf{S}^{\mathrm{T}} = \begin{bmatrix} \dfrac{\partial}{\partial x} & 0 & \dfrac{\partial}{\partial y} \\ 0 & \dfrac{\partial}{\partial y} & \dfrac{\partial}{\partial x} \end{bmatrix}, \quad \boldsymbol{\sigma}' = [\sigma'_x \;\; \sigma'_y \;\; \sigma_{xy}]^{\mathrm{T}}, \quad \mathbf{m} = [1 \;\; 1 \;\; 0]^{\mathrm{T}} \tag{4}$$

$\nabla^{\mathrm{T}} = [\partial/\partial x, \partial/\partial y]$ is the two-dimensional gradient operator, $\mathbf{v}$ the velocity of the solid skeleton, p the pore pressure in the fluid, ρ_m the mixture's density, $\mathbf{b}$ the body force vector, $\mathrm{d}\mathbf{v}/\mathrm{d}t$ the material time derivative of the velocity $\mathbf{v}$, k the Darcy permeability coefficient of the soil skeleton (assumed to be isotropic), $1/Q^*$ characterizes the compressibility of the mixture composed of the solid grains and the pore fluid,

$$\frac{1}{Q^*} = \frac{n}{K_f} + \frac{1-n}{K_s} \tag{5}$$

where n is the porosity, K_s and K_f are the bulk moduli of the solid particles and the pore fluid, respectively.

DOI: 10.1002/nag

Finally, the stress and the strain measures can be related by a suitable constitutive law in rate form. If the material behavior is rate-independent, it can be expressed as

$$\mathrm{d}\boldsymbol{\sigma}' = \mathbf{D}_{\mathrm{T}}\,\mathrm{d}\boldsymbol{\varepsilon} \tag{6}$$

where $\mathrm{d}\boldsymbol{\sigma}'$ is the rate of $\boldsymbol{\sigma}'$, $\mathrm{d}\boldsymbol{\varepsilon}$ is the vector form of the rate of deformation tensor, and $\mathbf{D}_{\mathrm{T}}$ is consistent tangent modulus matrix characterizing the constitutive behavior of the solid skeleton.

3. PRESSURE-STABILIZED GOVERNING EQUATIONS FOR SATURATED SOIL DYNAMICS

Governing equations (1) and (2) of saturated soil dynamics can be re-written as

$$\frac{\mathrm{d}\mathbf{v}}{\mathrm{d}t} - \frac{1}{\rho_m}\mathbf{S}^{\mathrm{T}}\mathbf{D}\mathbf{S}\mathbf{v} - \frac{1}{\rho_m}\mathbf{S}^{\mathrm{T}}\mathbf{m}\mathbf{p} + \frac{1}{\rho_m}\nabla p - \mathbf{b} = \mathbf{0} \tag{7}$$

$$\nabla^{\mathrm{T}}\mathbf{v} = \nabla^{\mathrm{T}}(k\nabla p) - \frac{\dot{p}}{Q^*} \tag{8}$$

As it is mentioned above the FIC process is a general stabilization method to eliminate numerical instabilities stemming from different sources. Nevertheless it is remarked that the purpose of the FIC process introduced in this work is to reformulate the mass conservation equation (8) for retaining incompressibility stabilization.

The essential difference of the FIC process with the standard infinitesimal calculus (SIC) process is, instead of considering an infinitesimal control volume, to consider a control volume with finite dimensions at the stage where the conservation equation, for instance, the mass conservation equation is given. Consequently, the variation of the physical variable with respect to spatial dimensions in the conservation equation should be expanded one higher order by Taylor series. In light of the FIC process, the original mass conservation equation (8) is then re-formulated as the stabilized one given below

$$r^d - \tfrac{1}{2}\mathbf{h}^{d^{\mathrm{T}}}\nabla r^d = 0 \quad \text{in } \boldsymbol{\Omega} \tag{9}$$

with

$$r^d = \nabla^{\mathrm{T}}\mathbf{v} - \nabla^{\mathrm{T}}(k\nabla p) + \frac{\dot{p}}{Q^*} \tag{10}$$

represents the residual of the mass conservation equation (8) of the mixture, $\mathbf{h}^d$ are the dimensions of the finite domain over which the balance of mass is enforced. Oñate [19] suggested to choose the parameters $\mathbf{h}^d$ in the form as below

$$\mathbf{h}^d = -2\lambda^d\mathbf{v} \tag{11}$$

In the above equation, the parameter λ^d is termed 'intrinsic time' per unit volume whose determination will be given later. The negative sign introduced in Equation (11) is necessary to ensure a positive stabilization in the mass balance equation at the discrete level. Substitution of Equation (11) into Equation (9) gives

$$r^d + \lambda^d\mathbf{v}^{\mathrm{T}}\nabla r^d = 0 \quad \text{in } \boldsymbol{\Omega} \tag{12}$$

DOI: 10.1002/nag

From the chain rule of differentiation, we can write

$$\mathbf{v}^{\mathrm{T}}\nabla r^d = \nabla^{\mathrm{T}}(r^d\mathbf{v}) - r^d\nabla^{\mathrm{T}}\mathbf{v} \tag{13}$$

Substitution of Equation (10) into Equation (13) and neglecting higher-order terms give

$$\mathbf{v}^{\mathrm{T}}\nabla r^d \approx \nabla^{\mathrm{T}}((\nabla^{\mathrm{T}}\mathbf{v})\mathbf{v}) + \nabla^{\mathrm{T}}\left(\mathbf{v}\left(-\nabla^{\mathrm{T}}(k\nabla p) + \frac{\dot{p}}{Q^*}\right)\right) \tag{14}$$

A combination of Equations (7) and (8) gives

$$(\nabla^{\mathrm{T}}\mathbf{v})\mathbf{v} = \left(\nabla^{\mathrm{T}}(k\nabla p) - \frac{\dot{p}}{Q^*}\right)\mathbf{v} - \left(\frac{\mathrm{d}\mathbf{v}}{\mathrm{d}t} - \frac{1}{\rho_m}\mathbf{S}^{\mathrm{T}}\mathbf{D}\mathbf{S}\mathbf{v} - \frac{1}{\rho_m}\mathbf{S}^{\mathrm{T}}\mathbf{m}p + \frac{1}{\rho_m}\nabla p - \mathbf{b}\right) \tag{15}$$

With substitution of Equations (10), (14) and (15) into Equation (12), the FIC stabilized form of the mass conservation equation is expressed as

$$\nabla^{\mathrm{T}}\mathbf{v} - \underline{\lambda^d\nabla^{\mathrm{T}}\left(\frac{\mathrm{d}\mathbf{v}}{\mathrm{d}t} - \frac{1}{\rho_m}\mathbf{S}^{\mathrm{T}}\mathbf{D}\mathbf{S}\mathbf{v} - \frac{1}{\rho_m}\mathbf{S}^{\mathrm{T}}\mathbf{m}p + \frac{1}{\rho_m}\nabla p - \mathbf{b}\right)} = \nabla^{\mathrm{T}}(k\nabla p) - \frac{\dot{p}}{Q^*} \tag{16}$$

The terms underlined in the above equation are the stabilization terms introduced by the FIC process, initially proposed by Oñate, who also suggested a suitable value for the stabilization parameter λ^d. It should be remarked that the term underlined in equation (16) is the divergence of the momentum conservation equation (7) multiplied by λ^d that is the one proposed by Hafez and Soliman to obtain stabilized continuity equation in the domain of computational fluid dynamics (CFD) in light of the penalty method modifying original continuity equation with a stabilized term of Laplacian of the pressure balanced using the divergence of the momentum equations [21]. The coincidence of Equation (16) in its structure with that obtained by Hafez and Soliman in CFD further justifies the validity of the proposed pressure-stabilized governing equations for saturated soil dynamics.

Obviously, the terms underlined involve the calculation of the third-order derivatives of the velocity vector that makes the linear finite elements inapplicable. To avoid such a calculation an additional vectorial variable $\boldsymbol{\varphi}$, which represents the summation of all the terms in the left-hand side of Equation (7) except the pressure gradient term, is introduced, i.e.

$$\boldsymbol{\varphi} = \frac{\mathrm{d}\mathbf{v}}{\mathrm{d}t} - \frac{1}{\rho_m}\mathbf{S}^{\mathrm{T}}\mathbf{D}\mathbf{S}\mathbf{v} - \frac{1}{\rho_m}\mathbf{S}^{\mathrm{T}}\mathbf{m}p - \mathbf{b} \tag{17}$$

From Equation (7) we have

$$\boldsymbol{\varphi} + \frac{1}{\rho_m}\nabla p = \mathbf{0} \tag{18}$$

Substitution of Equation (17) into Equation (16) results in

$$\nabla^{\mathrm{T}}\mathbf{v} - \lambda^d\nabla^{\mathrm{T}}\left(\boldsymbol{\varphi} + \frac{1}{\rho_m}\nabla p\right) = \nabla^{\mathrm{T}}(k\nabla p) - \frac{\dot{p}}{Q^*} \tag{19}$$

The above equation is the stabilized form of the mass conservation equation, which is re-derived with the use of the proposed version of the FIC process. To distinguish with the standard forms (7) and (8) of governing equations of saturated soil dynamics, Equations (7), (19) and (18) are

DOI: 10.1002/nag

termed pressure-stabilized governing equations of saturated soil dynamics. They can be written in the matrix–vector form as

$$\mathbf{S}^{\mathrm{T}}\boldsymbol{\sigma}' - \nabla p + \rho_m \mathbf{b} - \rho_m \frac{\mathrm{d}\mathbf{v}}{\mathrm{d}t} = 0 \tag{20}$$

$$\nabla^{\mathrm{T}}\mathbf{v} - \lambda^d \nabla^{\mathrm{T}}\boldsymbol{\varphi} - \frac{\lambda^d}{\rho_m}\nabla^2 p = \nabla^{\mathrm{T}}(k\nabla p) - \frac{\dot{p}}{Q^*} \tag{21}$$

$$\boldsymbol{\varphi} + \frac{1}{\rho_m}\nabla p = \mathbf{0} \tag{22}$$

It is observed that the governing equation set (20)–(22) to be numerically solved later only involve the second-order derivatives owing to the introduction of the additional variable $\boldsymbol{\varphi}$.

It is remarked that substitution of Equation (22) into Equation (21) leads the stabilization term going away from Equation (21). It means that the proposed pressure-stabilized form (21) of the mass conservation subjected to the constraint (22) is consistent with the standard mass conservation equation (8) in the continuous case and will consequently ensure that the solutions resulting from the discretized form of Equations (20)–(22) will satisfy the mass conservation condition. On the other hand, it should be stressed that the stabilization term will no longer disappear once Equations (22) and (21) are discretized as pointed out by Codina [22] in the work for the pressure stability analysis of the classical fractional step method. Indeed it will be shown later by Equation (41) and further by Equation (51) in the case of both impermeable and incompressible limits that the discretized form of Equation (21) in the spatial domain will result in generation of a stabilization term relating to the stabilization term in Equations (21) and (22).

4. THE ITERATIVE PRESSURE-STABILIZED FRACTIONAL STEP ALGORITHM (PS-IFSA)

The FSA is based on introducing an operator split procedure in temporal discretization of governing Equations (20)–(22) before spatial discretization.

Let us introduce an intermediate velocity $\mathbf{v}^*$ within a typical incremental time step $I_n \in [t_n, t_{n+1}]$ with $\Delta t = t_{n+1} - t_n$. The equilibrium equation (20) can then be split into the following two equations:

$$\rho_m \frac{\mathbf{v}^* - \mathbf{v}^n}{\Delta t} = \mathbf{S}^{\mathrm{T}}\boldsymbol{\sigma}'^{n+\theta_2} + \rho_m \mathbf{b} - \gamma \nabla p^n \tag{23}$$

$$\rho_m \frac{\mathbf{v}^{n+1} - \mathbf{v}^*}{\Delta t} = -\nabla(p^{n+\theta_2} - \gamma p^n) \tag{24}$$

with $0 < \theta_2 \leqslant 1$. In the above $\gamma = 0, 1$ corresponds to non-incremental and incremental versions of the split algorithm, respectively, and

$$p^{n+\theta_2} = p^n + \theta_2 \Delta p = p^n + \theta_2(p^{n+1} - p^n) \tag{25}$$

$$\boldsymbol{\sigma}'^{n+\theta_2} = \boldsymbol{\sigma}'^{n+\theta_2}(\mathbf{u}^{n+\theta_2}) \tag{26}$$

$$\mathbf{u}^{n+\theta_2} = \mathbf{u}^n + \theta_2 \Delta t[\theta_2 \mathbf{v}^{n+1} + (2-\theta_2)\mathbf{v}^n]/2 \tag{27}$$

DOI: 10.1002/nag

It is noted that all the pressure gradient, even the known pressure gradient at the previous time level, is removed from the first step shown by Equation (23) to enhance the stability of the FSA relating to the LBB condition. The scheme with this character is termed as the non-incremental version of the FSA.

The discretization of Equations (21) and (22) within the time sub-interval I_n can be written as

$$\frac{1}{Q^*}\frac{\Delta p}{\Delta t}=\nabla^{\mathrm{T}}\left[\left(\frac{\lambda^d}{\rho_m}+k\right)\nabla p^{n+\theta_1}\right]+\lambda^d\nabla^T\boldsymbol{\varphi}^{n+\theta_1}-\nabla^{\mathrm{T}}\mathbf{v}^{n+\theta_1} \tag{28}$$

$$\boldsymbol{\varphi}^{n+\theta_3}+\frac{1}{\rho_m}\nabla p^{n+\theta_3}=\mathbf{0} \tag{29}$$

with $0<\theta_1,\ \theta_3\leqslant 1$, where

$$\mathbf{v}^{n+\theta_1}=\mathbf{v}^n+\theta_1\Delta\mathbf{v}=(1-\theta_1)\mathbf{v}^n+\theta_1\mathbf{v}^{n+1} \tag{30}$$

$$p^{n+\theta_1}=p^n+\theta_1\Delta p=(1-\theta_1)p^n+\theta_1 p^{n+1} \tag{31}$$

$$\boldsymbol{\varphi}^{n+\theta_1}=\boldsymbol{\varphi}^n+\theta_1\Delta\boldsymbol{\varphi}=(1-\theta_1)\boldsymbol{\varphi}^n+\theta_1\boldsymbol{\varphi}^{n+1} \tag{32}$$

$$p^{n+\theta_3}=p^n+\theta_3\Delta p=(1-\theta_3)p^n+\theta_3 p^{n+1} \tag{33}$$

$$\boldsymbol{\varphi}^{n+\theta_3}=\boldsymbol{\varphi}^n+\theta_3\Delta\boldsymbol{\varphi}=(1-\theta_3)\boldsymbol{\varphi}^n+\theta_3\boldsymbol{\varphi}^{n+1} \tag{34}$$

With the substitution of Equation (24) into Equation (28), Equations (23), (28), (29), (24) can be re-written in the following form for the successive solution procedure in the FSA

$$\mathbf{v}^*=\mathbf{v}^n+\frac{\Delta t}{\rho_m}[(\mathbf{S}^{\mathrm{T}}\boldsymbol{\sigma}'^{n+\theta_2}+\rho_m\mathbf{b})-\gamma\nabla p^n] \tag{35}$$

$$\left[\frac{1}{Q^*}\frac{1}{\Delta t}-\theta_1\left(\frac{\lambda^d}{\rho_m}+k\right)\nabla^2-\frac{\Delta t}{\rho_m}\theta_1\theta_2\nabla^2\right]\Delta p=\nabla^{\mathrm{T}}\left(\frac{\lambda^d}{\rho_m}+k\right)\nabla p^n+\frac{\Delta t}{\rho_m}\theta_1\nabla^2 p^n+\lambda^d\nabla^T\boldsymbol{\varphi}^{n+\theta_1}$$
$$-\nabla^{\mathrm{T}}\mathbf{v}^n-\theta_1\nabla^{\mathrm{T}}(\mathbf{v}^*-\mathbf{v}^n)-\frac{\Delta t\theta_1}{\rho_m}\gamma\nabla^2 p^n \tag{36}$$

$$\Delta\boldsymbol{\varphi}=-\frac{1}{\theta_3}\left[\boldsymbol{\varphi}^n+\frac{1}{\rho_m}\nabla p^{n+\theta_3}\right] \tag{37}$$

$$\mathbf{v}^{n+1}=\mathbf{v}^*-\frac{\Delta t}{\rho_m}\nabla(p^{n+\theta_2}-\gamma p^n) \tag{38}$$

Equations (35)–(38) are then discretized in the space domain by applying standard Galerkin procedures. The field variables $\mathbf{v}$, p, $\boldsymbol{\varphi}$ are spatially approximated using shape functions $\mathbf{N}_u$, $\mathbf{N}_p$ in terms of their nodal values $\bar{\mathbf{v}}$,$\bar{\mathbf{p}}$, $\bar{\boldsymbol{\varphi}}$ as

$$\mathbf{v}=\mathbf{N}_u\bar{\mathbf{v}},\quad p=\mathbf{N}_p\bar{\mathbf{p}},\quad \boldsymbol{\varphi}=\mathbf{N}_u\bar{\boldsymbol{\varphi}} \tag{39}$$

DOI: 10.1002/nag

and we arrive to

$$\bar{\mathbf{v}}^* = \bar{\mathbf{v}}^n + \Delta t \mathbf{M}^{-1}\left(\mathbf{f}_u^{n+\theta_2} + \mathbf{R}^{n+\theta_2} + \int_{\Gamma_p} \mathbf{N}_u^{\mathrm{T}} \mathbf{p}^{n+\theta_2}\,\mathrm{d}\Gamma - \int_{\Omega} \mathbf{B}^{\mathbf{T}} \boldsymbol{\sigma}'^{n+\theta_2}\,\mathrm{d}\Omega - \gamma \mathbf{G}_p \bar{\mathbf{p}}^n\right) \tag{40}$$

$$\left(\frac{1}{\Delta t}\tilde{\mathbf{S}} + \theta_1 \mathbf{H} + \Delta t \theta_1 \theta_2 \mathbf{H}^*\right)\Delta \bar{\mathbf{p}} = \mathbf{f}_p^{n+\theta_1} - \mathbf{H}\bar{\mathbf{p}}^n - \Delta t \theta_1 (1-\gamma)\mathbf{H}^* \bar{\mathbf{p}}^n - \lambda^d \mathbf{D}\bar{\boldsymbol{\varphi}}^{n+\theta_1} - \mathbf{Q}^{\mathrm{T}}\bar{\mathbf{v}}^n + \theta_1 \mathbf{G}_p^{\mathrm{T}} \Delta \bar{\mathbf{v}}^* - \theta_1 \int_{\Gamma_q + \Gamma_p} \mathbf{N}_p^{\mathrm{T}} \Delta \bar{\mathbf{v}}^n\,\mathrm{d}\Gamma \tag{41}$$

$$\Delta \bar{\boldsymbol{\varphi}} = -\frac{1}{\theta_3}[\bar{\boldsymbol{\varphi}}^n + \mathbf{M}^{-1}\mathbf{G}_p \bar{\mathbf{p}}^{n+\theta_3}] \tag{42}$$

$$\bar{\mathbf{v}}^{n+1} = \bar{\mathbf{v}}^* - \Delta t \mathbf{M}^{-1}\mathbf{G}_p(\bar{\mathbf{p}}^{n+\theta_2} - \gamma \bar{\mathbf{p}}^n) \tag{43}$$

where $\Delta \bar{\mathbf{v}}^* = \bar{\mathbf{v}}^* - \bar{\mathbf{v}}^n$, $\Delta \bar{\mathbf{v}}^n = \bar{\mathbf{v}}^{n+1} - \bar{\mathbf{v}}^n$, $\mathbf{B}$ is the strain–displacement matrix, Γ_q and Γ_p are the parts of the boundary on which the pore fluid flux and pore pressures are prescribed, respectively, and

$$\begin{aligned}
\mathbf{M} &= \int_{\Omega} \mathbf{N}_u^{\mathrm{T}} \rho_m \mathbf{N}_u\,\mathrm{d}\Omega, \quad \mathbf{H} = \int_{\Omega} (\nabla \mathbf{N}_p)^{\mathrm{T}} \left(\frac{\lambda^d}{\rho_m} + k\right)(\nabla \mathbf{N}_p)\,\mathrm{d}\Omega \\
\tilde{\mathbf{S}} &= \int_{\Omega} \mathbf{N}_p^{\mathrm{T}} \frac{1}{Q^*} \mathbf{N}_p\,\mathrm{d}\Omega, \quad \mathbf{Q} = \int_{\Omega} \mathbf{B}^{\mathrm{T}} m \mathbf{N}_p\,\mathrm{d}\Omega \\
\mathbf{H}^* &= \int_{\Omega} (\nabla \mathbf{N}_p)^{\mathrm{T}} \frac{1}{\rho_m}(\nabla \mathbf{N}_p)\,\mathrm{d}\Omega, \quad \mathbf{G}_p = \int_{\Omega} \mathbf{N}_u^{\mathrm{T}} \nabla \mathbf{N}_p\,\mathrm{d}\Omega \\
\mathbf{f}_u^{n+\theta_2} &= (1-\theta_2)\mathbf{f}_u^n + \theta_2 \mathbf{f}_u^{n+1}, \quad \mathbf{R}^{n+\theta_2} = \int_{\Gamma_t} \mathbf{N}_u^{\mathrm{T}} \boldsymbol{\sigma}^{n+\theta_2} \cdot \mathbf{n}\,\mathrm{d}\Gamma \\
\mathbf{f}_p &= \int_{\Gamma_q} \mathbf{N}_p^{\mathrm{T}} k \frac{\partial p}{\partial n}\,\mathrm{d}\Gamma, \quad \mathbf{D} = \int_{\Omega} (\nabla \mathbf{N}_p)^{\mathrm{T}} \mathbf{N}_u\,\mathrm{d}\Omega
\end{aligned} \tag{44}$$

in which $\mathbf{f}_u^n$ and $\mathbf{f}_u^{n+1}$ are the external force vectors at time t_n and t_{n+1}, respectively. Equations (40)–(43), which reduce to the form of IFAS while λ_d goes to zero, constitute the discretized system of the proposed PS-IFSA.

It is shown that to solve Equation (40) for $\bar{\mathbf{v}}^*$ both the pore pressure $p^{n+\theta_2}$ and the effective stress $\boldsymbol{\sigma}'^{n+\theta_2}$, depending on the displacements at time $t_{n+\theta_2}$ are required and obviously should be determined in an iterative way. On the other hand, it also implies that the momentum conservation equation is satisfied in an implicit sense and therefore the stability of the proposed algorithm in the time domain is enhanced. Indeed, the introduction of the iterative procedure into the proposed PS-FSA allows much larger time step sizes to be used than those limited in existing explicit and semi-implicit ones and results in saving the computational effort in a decisive manner. For a typical

DOI: 10.1002/nag

incremental time step $I_n \in [t_n, t_{n+1}]$, the proposed PS-IFSA can be summarized as follows:

(1) assume $\bar{\mathbf{v}}_{(0)}^{n+1} \Leftarrow \bar{\mathbf{v}}^n$, $\bar{\boldsymbol{\varphi}}_{(0)}^{n+1} \Leftarrow \bar{\boldsymbol{\varphi}}^n$, $\bar{\mathbf{p}}_{(0)}^{n+1} = \bar{\mathbf{p}}^n$, $\boldsymbol{\sigma}_{(0)}'^{n+1} = \boldsymbol{\sigma}'^n$ as the initial predictor, let the iteration number $i \Leftarrow 1$ for the satisfaction of the momentum conservation;
(2) use Equation (27) to compute the nodal displacements $\bar{\mathbf{u}}_{(i-1)}^{n+\theta_2} = \bar{\mathbf{u}}^n + \theta_2 \Delta t[\theta_2 \bar{\mathbf{v}}_{(i-1)}^{n+1} + (2-\theta_2)\bar{\mathbf{v}}^n]/2$ at time $t_{n+\theta_2}$, then determine $\boldsymbol{\sigma}_{(i-1)}'^{n+\theta_2}(\bar{\mathbf{u}}_{(i-1)}^{n+\theta_2})$ according to the constitutive law used to describe the linear or non-linear behavior of the solid skeleton and use it to solve for $\bar{\mathbf{v}}^*$ by Equation (40);
(3) let $\bar{\boldsymbol{\varphi}}_{(i,0)}^{n+1} \Leftarrow \bar{\boldsymbol{\varphi}}_{(i-1)}^{n+1}$ and the number of iterations for the variable $\bar{\boldsymbol{\varphi}}^{n+1}$ $j \Leftarrow 1$;
(4) solve Equation (41) to determine $\Delta\bar{\mathbf{p}}$ (then $\bar{\mathbf{p}}^{n+1}$) by using $\bar{\mathbf{v}}^*$, $\bar{\mathbf{p}}^n$ and $\bar{\boldsymbol{\varphi}}_{(i,j-1)}^{n+1}$;
(5) solve Equation (42) to determine $\bar{\boldsymbol{\varphi}}_{(i,j)}^{n+1}$ by using $\bar{\mathbf{p}}^{n+1}$;
(6) check for convergence of the jth iteration for the variable $\bar{\boldsymbol{\varphi}}^{n+1}$, if $\|\boldsymbol{\varphi}_{(i,j)}^{n+1} - \boldsymbol{\varphi}_{(i,j-1)}^{n+1}\|_\infty \leqslant \varepsilon_1$, let $\bar{\boldsymbol{\varphi}}^{n+1} \Leftarrow \bar{\boldsymbol{\varphi}}_{(i,j)}^{n+1}$ and terminate the iteration loop, otherwise $j \Leftarrow j+1$ and go to (4);
(7) solve Equation (43) to determine $\bar{\mathbf{v}}_{(i)}^{n+1}$ by using $\bar{\mathbf{v}}^*$, $\bar{\mathbf{p}}^n$ and $\bar{\mathbf{p}}^{n+1}$;
(8) check for convergence of the ith iteration, if $\|\bar{\mathbf{v}}_{(i)}^{n+1} - \bar{\mathbf{v}}_{(i-1)}^{n+1}\|_\infty \leqslant \varepsilon_2$, terminate the ith iteration loop, otherwise $i \Leftarrow i+1$ and go to (2).

5. PRESSURE STABILITY ANALYSIS

The effect of the FIC process for the pressure stabilization introduced into the proposed PS-IFSA can be demonstrated by the following pressure stability analysis.

It is noted that if the soil permeability is zero and both the solid grains and the pore water are incompressible, we will have in Equation (41) that

$$\mathbf{f}_p = 0, \quad \mathbf{H} = \lambda^d \mathbf{H}^*, \quad \tilde{\mathbf{S}} = \mathbf{0} \tag{45}$$

In addition, the boundary term shown as the last term at the right-hand side of Equation (41) can be assumed to be zero following Codina *et al.* [23], i.e.

$$-\theta_1 \int_{\Gamma_q + \Gamma_p} \mathbf{N}_p^{\mathrm{T}} \Delta\bar{\mathbf{v}}^n \, \mathrm{d}\Gamma = \mathbf{0} \tag{46}$$

Substitution of Equations (45) and (46) into Equation (41) results in

$$(\Delta t \theta_1 \theta_2 + \theta_1 \lambda^d)\mathbf{H}^* \Delta\bar{\mathbf{P}} = -[\Delta t \theta_1 (1-\gamma) + \lambda^d]\mathbf{H}^* \bar{\mathbf{P}}^n - \lambda^d \mathbf{D}\bar{\boldsymbol{\varphi}}^{n+\theta_1} - \mathbf{Q}^{\mathrm{T}}\bar{\mathbf{v}}^n + \theta_1 \mathbf{G}_p^{\mathrm{T}} \Delta\bar{\mathbf{v}}^* \tag{47}$$

From Equation (42) the term $\bar{\boldsymbol{\varphi}}^{n+\theta_1}$ required in Equation (47) can be given by

$$\bar{\boldsymbol{\varphi}}^{n+\theta_1} = \bar{\boldsymbol{\varphi}}^n + \theta_1 \Delta\bar{\boldsymbol{\varphi}} = \left(1 - \frac{\theta_1}{\theta_3}\right)\bar{\boldsymbol{\phi}}^n - \frac{\theta_1}{\theta_3}\mathbf{M}^{-1}\mathbf{G}_p \bar{\mathbf{p}}^{n+\theta_3} \tag{48}$$

Equation (43) can be re-written in the form

$$\Delta\bar{\mathbf{v}}^* = \Delta\bar{\mathbf{v}}^n + \Delta t \mathbf{M}^{-1}\mathbf{G}_p(\bar{\mathbf{p}}^{n+\theta_2} - \gamma\bar{\mathbf{p}}^n) \tag{49}$$

DOI: 10.1002/nag

Substitution of Equations (48) and (49) into Equation (47) with noticing that [15]

$$\mathbf{G}_p^{\mathrm{T}}\Delta\bar{\mathbf{v}}^n = -\mathbf{Q}^{\mathrm{T}}\Delta\bar{\mathbf{v}}^n \tag{50}$$

results in

$$\mathbf{Q}^{\mathrm{T}}\bar{\mathbf{v}}^{n+\theta_1} + \Delta t\theta_1(\mathbf{H}^* - \mathbf{G}_p^{\mathrm{T}}\mathbf{M}^{-1}\mathbf{G}_p)(\bar{\mathbf{p}}^{n+\theta_2} - \gamma\bar{\mathbf{p}}^n) + \lambda^d\left(\mathbf{H}^*\bar{\mathbf{p}}^{n+\theta_1} - \frac{\theta_1}{\theta_3}\mathbf{D}\mathbf{M}^{-1}\mathbf{D}^{\mathrm{T}}\bar{\mathbf{p}}^{n+\theta_3}\right) = -\lambda^d\mathbf{D}\left(1 - \frac{\theta_1}{\theta_3}\right)\bar{\boldsymbol{\varphi}}^n \tag{51}$$

in which the parameters θ_1, θ_2, θ_3 used, respectively, for the discretizations of momentum and mass balance equations and additional equation of the FIC procedure in the time domain are allowed to be different. For simplicity, we use the unique value of θ_1, θ_2, θ_3 equal to 0.5 for the numerical examples in the present paper.

It is important to note that in the case of that the soil permeability is zero and both the solid grains and pore water are assumed incompressible the spatial discretization of the original mass conservation equation (8) should be written as

$$\mathbf{Q}^{\mathrm{T}}\bar{\mathbf{v}}^{n+\theta_1} = \mathbf{0} \tag{52}$$

It implies that the spatial discretization of original governing equations (7) and (8) of saturated soil dynamics will result in a set of mixed formulations with null diagonal sub-matrix that is a characteristic of problem constrained by a Lagrange multiplier variable and bring more severe restriction imposed by the LBB condition in the shape functions for velocity–pressure interpolations. It is seen from Equations (50) and (51) that the proposed PS-FSA is stabilized by means of introducing the two stabilization terms into Equation (52), consequently the $\bar{\mathbf{v}}-\bar{\mathbf{p}}$ mixed formulation becomes irreducible, i.e. without null diagonal sub-matrix. The two stabilization terms are symbolized as

$$\boldsymbol{\Psi}_1 = \Delta t\theta_1(\mathbf{H}^* - \mathbf{G}_p^{\mathrm{T}}\mathbf{M}^{-1}\mathbf{G}_p)(\bar{\mathbf{p}}^{n+\theta_2} - \gamma\bar{\mathbf{p}}^n) \tag{53}$$

$$\boldsymbol{\Psi}_2 = \lambda^d\left(\mathbf{H}^*\bar{\mathbf{p}}^{n+\theta_1} - \frac{\theta_1}{\theta_3}\mathbf{D}\mathbf{M}^{-1}\mathbf{D}^{\mathrm{T}}\bar{\mathbf{p}}^{n+\theta_3}\right) \tag{54}$$

Obviously $\boldsymbol{\Psi}_1$ is only introduced as the stabilization term in the standard FSA, for which $\lambda^d = 0$ and therefore $\boldsymbol{\Psi}_2 = 0$. It is observed that the pressure stability contributed by the term $\boldsymbol{\Psi}_1$ is weak for the standard FSA, since it is explicit in nature and hence small time step size Δt has to be taken due to the conditional stability of the explicit time-stepping process. This explains why the introduction of an iterative procedure into the standard FSA enables to enhance the pressure stability [17], as the introduced iterative procedure makes both stresses and pressure terms satisfy the momentum conservation equation in an implicit sense.

It should also be stressed that if the incremental version ($\gamma = 1$), instead of the non-incremental version ($\gamma = 0$), is chosen in the standard FSA, the pressure stability will be extremely weak as in this case the term $\boldsymbol{\Psi}_1$ is a small quantity of order $O(\Delta t^2)$. Especially as one concerns with steady-state problems, i.e. $\bar{\mathbf{p}}^{n+\theta_2} - \bar{\mathbf{p}}^n \cong 0$, the first stabilization term $\boldsymbol{\Psi}_1 \to 0$ reaches and spurious oscillations will occur in the resulting pressure field.

The additional stabilized term $\boldsymbol{\Psi}_2$ with $\lambda^d \neq 0$ attributed to the FIC process enhances the stability of the proposed FSA. It is remarked that the stabilization term $\boldsymbol{\Psi}_2$ is proportional to the value

DOI: 10.1002/nag

of the parameter λ^d independent of the time step size used in the algorithm. A proper value of λ^d is chosen as the critical time step size Δt_{crit} determined by the conditional stability of explicit scheme [16, 24] that could be explained as below. The stabilization term $\boldsymbol{\Psi}_2$ introduced by the FIC process is similar in its vector structure to $\boldsymbol{\Psi}_1$ for the classical non-incremental FSA. It has been indicated that the classical non-incremental FSA possesses the best pressure stabilization as the time step size used can be allowed to increase to the critical time value determined in terms of the explicit time integration scheme. Therefore, we heuristically deduce that the intrinsic time λ^d should be assumed to be equal to the critical time step size. Here, it is necessary to emphasize that the purpose of this value (λ^d) is only used as one term to determine the length scale in the FIC process, i.e. $h_j^d = -2\lambda^d v_j$, which determine the control volume and over which the balance of mass is enforced. It is not related to the time step restriction of the proposed algorithm.

Thanks to the independence of the stability contributed by the term $\boldsymbol{\Psi}_2$ from the time step size Δt taken for a particular problem, the proposed PS-IFSA can be applied to simulate a variety of dynamic behaviors of saturated porous media ranging from quasi-static, slow to medium and high-speed motion phenomena. For quasi-static and slow motion phenomena, which are typical of the consolidation behavior of soils, relative large time step size should be used to enhance the computational efficiency while the computational accuracy required is still ensured. Whereas for the simulation of medium and high-speed phenomena, for instance for the problems of earthquake analysis and the problems subjected to impulse loads, where high-frequency responses dominate, extremely small time step has to be taken possibly to obtain reliable results and further to ensure computational accuracy.

Hence, the significance of the stabilization term $\boldsymbol{\Psi}_2$ is prominent and is particularly emphasized in the present paper for the example problems where extremely small time step size has to be taken since existing FSAs can only ensure numerical stability if the time step size larger than a critical value is used. This minimum time step size requirement may conflict with the maximum time step size limitation relative to the minimum wavelength in the simulation of dynamic response problems and leads to failure of existing FSAs to those problems.

6. NUMERICAL EXAMPLES

It has been demonstrated that the IFSA proposed in Reference [17] allows much larger time step sizes to be used than those limited in existing explicit and semi-implicit versions of the algorithm. The prominent performance of the IFSA in this aspect has been shown in [17] and will not be repeatedly demonstrated in this paper.

In this section we will limit ourselves to only demonstrate how the introduction of the FIC process into the IFSA, including non-incremental and incremental versions, improves their performances, namely, removes the dependence of the stability of the algorithms on the time step size, which allows much smaller time step sizes to be used than those used in existing FSAs and ensures the application of the algorithm to saturated soil dynamics problems with high frequencies, furthermore, allows using the incremental version of the algorithm.

The example considers the two-dimensional problem of a soil layer of 5 m deep lying on a rock bed. The saturated soil layer is subjected to a strip of uniformly distributed pressure load applied to the central 1 m section of the top surface as shown in Figure 1(a). The remaining of the top surface is assumed to be traction free. The geometry and the boundary conditions of the problem are also

DOI: 10.1002/nag

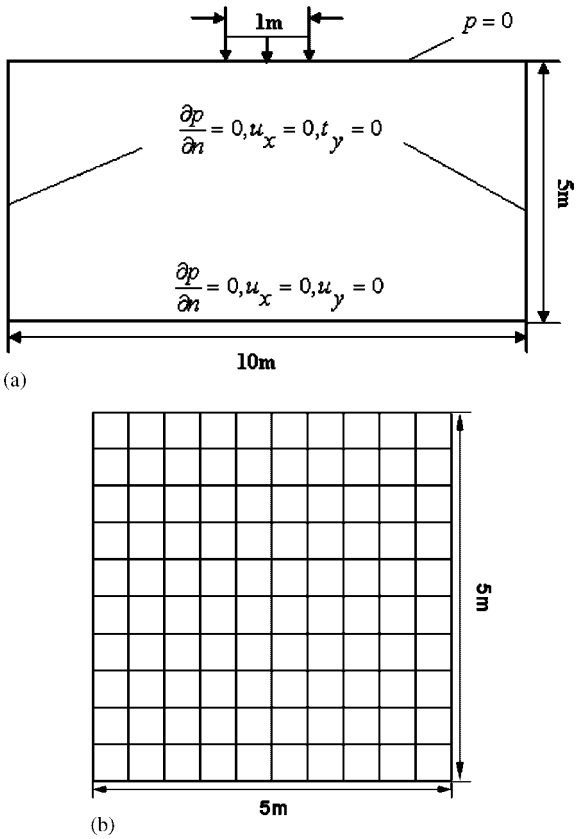

Figure 1. Geometry, boundary conditions and mesh of centrally loaded saturated soil strip. (a) Geometry and boundary conditions and (b) finite element mesh.

sketched in the same figure. Both horizontal and vertical components of displacements are taken as zero at the bottom. The computational domain is intercepted by two artificial boundaries in the horizontal directions, where horizontal displacements and vertical surface tractions are assumed to be zero. It is important to notice that in order to allow radiation of the waves generated inside the domain special radiation boundary conditions should be used. However, as the purpose of this example is just to show the performance of the proposed PS-IFSA, no radiation boundary condition is applied. The mesh is shown in Figure 1(b) in which, by symmetry, only one-half with 5 m wide of the computational domain is taken and discretized with a 10×10 element mesh. The horizontal and vertical displacements at the left boundary of the meshed domain are assumed as fixed and free, respectively, due to the symmetry condition. Concerning pore pressures, we prescribe the pore pressure at the top surface as zero, and assume the lateral and the bottom boundaries to be impermeable.

The four test cases for the example described above are selected to cover different dynamic responses in both elastic and elastoplastic saturated soil structures subjected to cyclic loads with high frequencies and the step loads.

DOI: 10.1002/nag

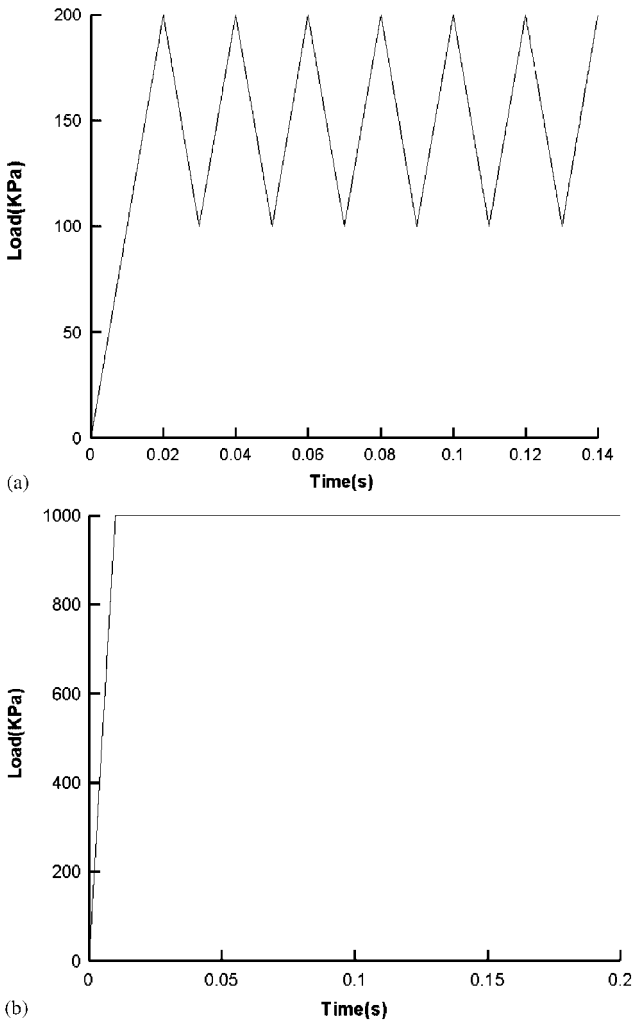

Figure 2. Loading histories for the saturated soil dynamics problem. (a) Cyclic loading with high frequency and (b) step loading with a ramp between $t=0$ and 0.01 s.

It should be noted that Q1Q1 quadrilateral (the 4-noded bi-linear quadrilateral for both displacements and pressures), which presents notable advantages in computational efficiency and the convenience of using adaptive re-meshing techniques, is used in this work to demonstrate the performance of the FSA in circumventing the restriction imposed by the LBB condition. To do it, the grains and water are assumed to be incompressible, i.e. $Q^* \to \infty$ and the permeability is assumed to be zero.

First, the soil skeleton is assumed elastic, with Young's modulus $E=1\times10^4$ kPa and Poisson's ratio $\gamma=0.2$. The density of the saturated soil mixture is $\rho_m=2000\,\mathrm{kg/m^3}$. The soil layer is subjected to a cyclic load with high frequency depicted in Figure 2(a).

DOI: 10.1002/nag

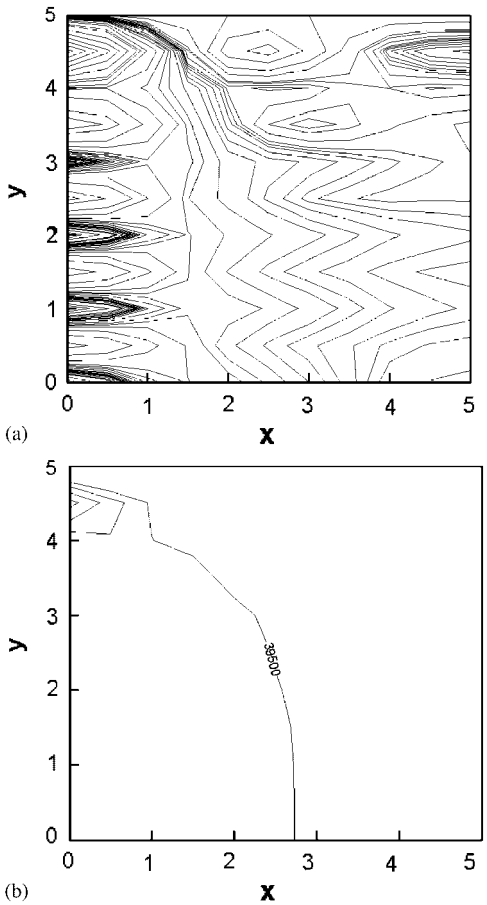

Figure 3. Pore pressure distributions at time $t=0.06$ s using Q1Q1 elements ($\Delta t=10^{-4}$ s). (a) IFSA-N and (b) proposed PS-IFSA-N.

As the first test case, the dynamic responses of the soil layer subjected to the cyclic load are performed with the two non-incremental versions of IFSA with and without the introduction of the FIC process, i.e. the proposed PS-IFSA-N and the existing IFSA-N to demonstrate crucial importance of the FIC process in retaining the pressure stability for the algorithm when the high-frequency responses dominate and small time step size has to be taken to ensure necessary computational accuracy. Figure 3 illustrates pore pressure contours obtained by both PS-IFSA-N and IFSA-N at time $t=0.06$ s as a time step size $\Delta t=10^{-4}$ s is used. It is observed that severe numerical oscillations occur in the pore pressure contours obtained by the IFSA-N as shown in Figure 3(a) while the resulting solutions of pore pressure obtained by the proposed PS-IFSA-N are stable without spurious oscillations in the spatial domain.

As it is widely accepted that the incremental versions of the algorithm will generally provide the results with high accuracy than those obtained by the non-incremental versions, the second concerns with the test case as same as the first test case in the material properties

DOI: 10.1002/nag

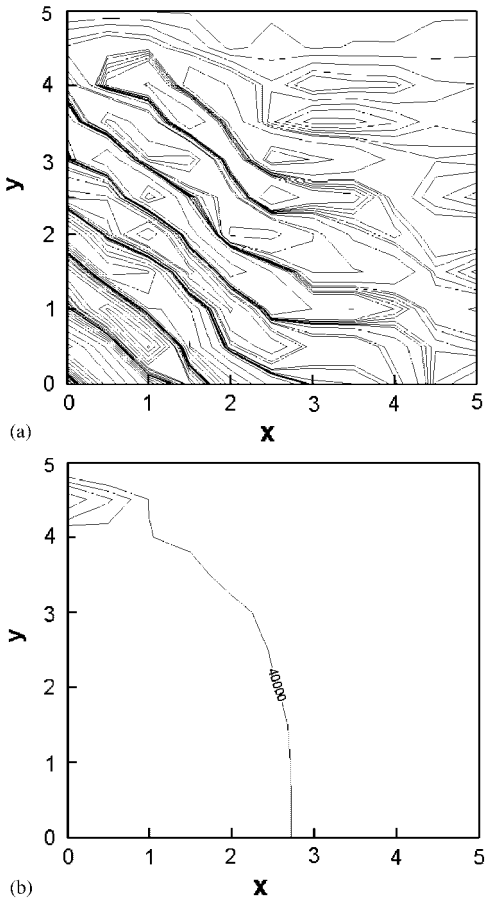

Figure 4. Pore pressure distributions at time $t = 0.06$ s using Q1Q1 elements ($\Delta t = 10^{-3}$ s). (a) IFSA-I and (b) proposed PS-IFSA-I.

and loading conditions but performed with the incremental versions PS-IFSA-I and IFSA-I of the algorithm, i.e. incremental IFSAs with and without the introduction of the FIC process, respectively.

It is shown in Figure 4(a) that even though $\Delta t = 10^{-3}$ s larger than that used in the first tested case is used, severe numerical oscillations still occur in the pore pressure contours given by the IFSA-I, whereas PS-IFSA-I performs well as shown in Figure 4(b) for the pressure contours due to the introduction of the FIC process.

To demonstrate the convergences of proposed PS-IFSA-I in both temporal and spatial domains, respectively, we consider, as the third test case, the test case for the same example performed by using the proposed PS-IFSA-I with the two sub-cases with different combinations of element mesh and time step size, i.e. (1) the 10×10 element mesh but a smaller time step size $\Delta t = 10^{-4}$ s and (2) the time step size $\Delta t = 10^{-3}$ s, but a refined 20×20 element mesh. The resulting pressure contours provided by the two sub-cases are given in Figure 5. It can be observed that the results agree very

DOI: 10.1002/nag

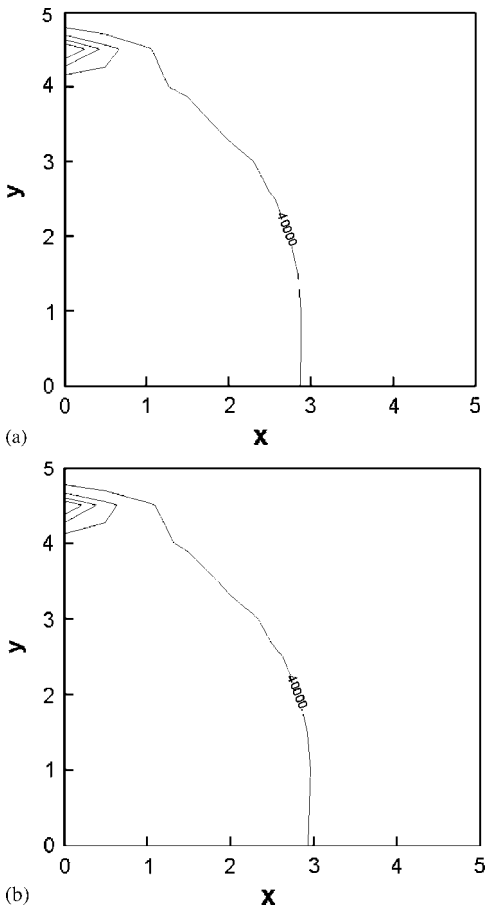

Figure 5. Pore pressure distributions at time $t=0.06$ s using Q1Q1 elements. (a) Proposed PS-IFSA-I with a 10×10 element mesh ($\Delta t=10^{-4}$ s) and (b) proposed PS-IFSA-I with a refined 20×20 element mesh ($\Delta t=10^{-3}$ s).

well with those shown in Figure 4(b) and good convergences of the proposed PS-IFSA-I in both temporal and spatial domains are obtained.

Finally, the fourth tested case of the example concerns the case where a more realistic, materially non-linear constitutive model is considered. We take the same example problem described above, but using now an elastoplastic constitutive model. All boundary conditions for displacements and pressures remain unchanged.

The strip of uniformly distributed pressure load applied to the top surface is now a step loading with a ramp between $t=0$ and 0.01 s, i.e. the load increases from 0 to 1000 kPa within 0.01 s at the first loading stage, and then remains constant through the analysis (the second loading stage) as showed in Figure 2(b). Concerning the soil model, we choose a non-associated Drucker–Prager model with hardening. The material constants are: (i) cohesion $c=10$ kPa, (ii) internal friction angle $\phi=35°$, (iii) the plastic potential is of Drucker–Prager type, with a plastic potential angle

DOI: 10.1002/nag

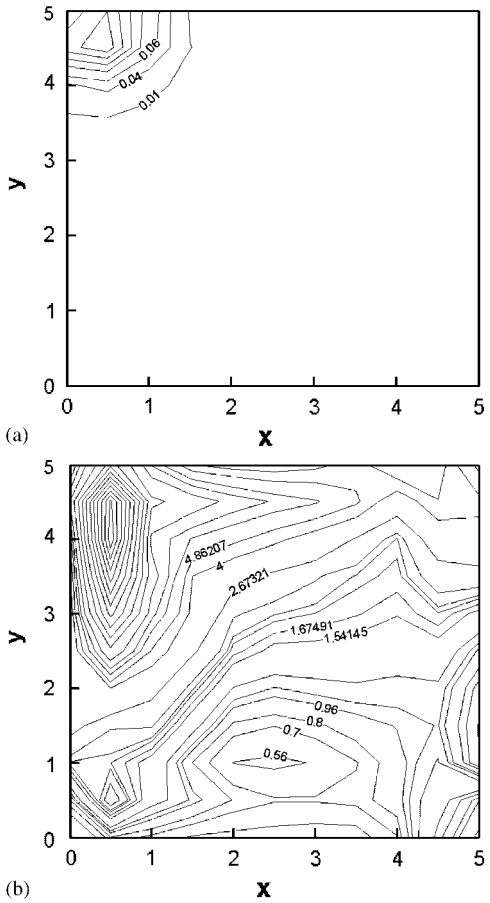

Figure 6. Equivalent plastic strain distributions using Q1Q1 elements and the IFSA-I ($\Delta t = 10^{-3}$ s). (a) $t = 0.2$ s and (b) $t = 0.1$ s.

$\phi = 12°$, (iv) strain hardening parameter $h = 10$ kPa. Figure 6(a) and (b) illustrate, respectively, the profiles of equivalent plastic strain at time $t = 0.01$ and 0.1 s obtained by the IFSA-I as $\Delta t = 10^{-3}$ s is used, from which we can see how the spurious oscillations develop along with time.

Then the test case is performed again with the proposed PS-IFSA-I using the same time step $\Delta t = 10^{-3}$ s. It is obviously observed from Figure 7(a) and (b) that no spurious oscillation occurs at time $t = 0.01$ and 0.1 s that demonstrate the validity of the proposed incremental, PS-IFSA.

7. CONCLUSIONS

The original fractional step algorithm (FSA) was introduced to circumvent the restrictions imposed by the LBB condition in the interpolation approximations of mixed formulations of the **u**–p model in saturated soil dynamics.

DOI: 10.1002/nag

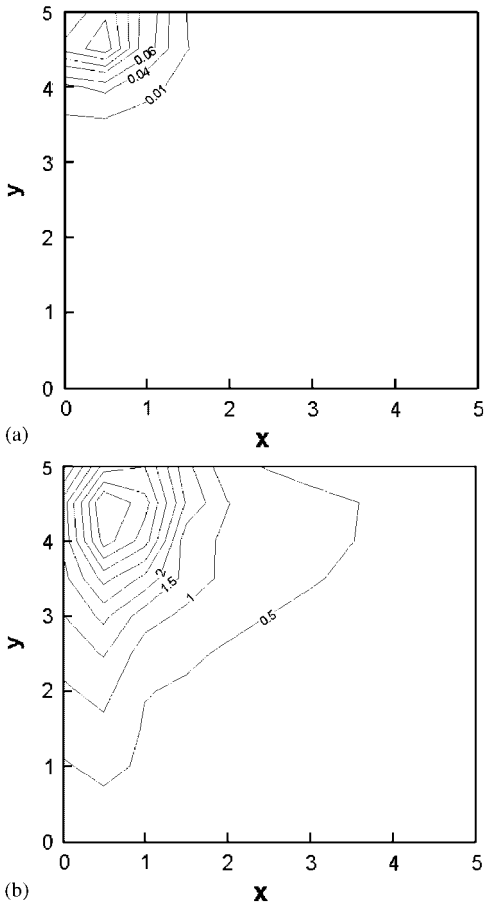

Figure 7. Equivalent plastic strain distributions using Q1Q1 elements and proposed PS-IFSA-I ($\Delta t = 10^{-3}$ s). (a) $t = 0.2$ s and (b) $t = 0.1$ s.

However, two serious disadvantages of the original FSA exist. One is over severe limitation of maximum time step size due to its explicit nature, which has been overcome by means of the introduction of an iterative procedure [17]. The other lies in its minimum time step size required and the non-incremental version of the algorithm required in order to ensure the stability of the algorithm relating to the LBB condition.

In the present paper, an improved new version of the FSA, i.e. the iterative pressure-stabilized FSA abbreviated as PS-IFSA is proposed by means of further introduction of the FIC process to the IFSA. The proposed PS-IFSA for saturated soil dynamics removes the minimum time step size bound and allows the use of the incremental version of the algorithm while the pressure stability still remains, thereby will be robust not only to the low-frequency response problems, for which large time step sizes should be used to enhance the computational efficiency, but also to the high-frequency response problems, for which small time step sizes have to be taken to fulfill necessary computational accuracy.

DOI: 10.1002/nag

ACKNOWLEDGEMENTS

The authors are pleased to acknowledge the support of this work by the National Natural Science Foundation of China through contract/grant numbers 10672033, 90715011 and 10590354 and the National Key Basic Research and Development Program (973 Program, No. 2010CB731502).

REFERENCES

1. Ladyshenskaya OA. *The Mathematical Theory of Viscous Incompressible Flow* (2nd edn). Gordon and Breach: New York, 1969.
2. Babuska I. The finite element method with Lagrange multiplier. *Numerische Mathematik* 1973; **20**:179–192.
3. Brezzi F. On the existence, uniqueness and approximation of saddle point problems arising from Lagrangian multipliers. *RAIRO 8-R2* 1974; 129–151.
4. Zienkiewicz OC, Qu S, Taylor RL, Nakzawa S. The patch test for mixed formulation. *International Journal for Numerical Methods in Engineering* 1986; **23**:1871–1883.
5. Zienkiewicz OC, Paul DK, Chan AHC. Unconditionally stable staggered solution procedure for soil–pore fluid interaction problems. *International Journal for Numerical Methods in Engineering* 1988; **26**:1039–1055.
6. Gresho PM, Sani RL, Engelman MS. *Incompressible Flow and the Finite Element Method*. Wiley: Chichester, England, 1998.
7. Chorin AJ. Numerical solution of the Navier–Stokes equations. *Mathematics of Computer* 1968; **22**:742–762.
8. Chorin AJ. On the convergence of discrete approximation to the Navier–Stokes equations. *Mathematics of Computer* 1969; **23**:341–353.
9. Schneider GE, Raithby GD, Yovanovich MM. Finite element analysis of incompressible flow incorporating equal order pressure and velocity interpolation. In *Numerical Methods for Laminar and Turbulent Flow*, Taylor C, Morgan K, Brebbia C (eds). Pentech Press: Plymouth, 1978.
10. Kawahara M, Ohmiya K. Finite element analysis of density flow using velocity correction method. *International Journal of Numerical Methods in Fluids* 1985; **5**:1135–1149.
11. de Sampaio PAB. A Petrov–Galerkin formulation for the incompressible Navier–Stokes equations using equal order of interpolation for velocity and pressure. *International Journal Numerical Methods in Engineering* 1991; **31**:1135–1149.
12. Zienkiewicz OC, Codina R, Morgan K, Satya Sai BVP. A general algorithm for compressible and incompressible for. Part I: the split characteristic based scheme. *International Journal of Numerical Methods in Fluids* 1995; **20**:869–885.
13. Pastor M, Zienkiewicz OC, Li T, Liu X, Huang M. Stabilized finite elements of equal order of interpolation for soil dynamic problems. *Archives of Computational Methods in Engineering* 1999; **6**:3–33.
14. Pastor M, Li T, Liu X, Zienkiewicz OC. Stabilized low-order elements for failure and localization problems in unsaturated soils and foundations. *Computer Methods in Applied Mechanics and Engineering* 1999; **174**:219–234.
15. Pastor M, Li T, Liu X, Zienkiewicz OC, Quecedo M. A fractional step algorithm allowing equal order of interpolation for coupled analysis of saturated soil problems. *Mechanics of Cohesive-Frictional Materials* 2000; **5**:511–534.
16. Codina R. Pressure stability in fractional step finite element methods for incompressible flows. *Journal of Computational Physics* 2001; **170**(1):112–140.
17. Li XK, Han XH, Pastor M. An iterative stabilized fractional step algorithm for finite element analysis in saturated soil dynamics. *Computer Methods in Applied Mechanics and Engineering* 2003; **192**:3845–3859.
18. Zienkiewicz OC, Taylor RL, Nithiarasu P. *The Finite Element Method for Fluid Dynamics* (6th edn). Elservier: Amsterdam, 2005.
19. Oñate E. A stabilized finite element method for incompressible viscous flows using a finite increment calculus formulation. *Computer Methods in Applied Mechanics and Engineering* 2000; **182**:355–370.
20. Zienkiewicz OC, Shiomi T. Dynamic behavior of saturated porous media: the generalized Biot formulation and its numerical solution. *International Journal for Numerical and Analytical Methods in Geomechanics* 1984; **8**:71–96.
21. Hafez M, Soliman M. Numerical solution of the incompressible Navier–Stokes equations in primitive variables on unstaggered grids. In *Incompressible Computational Fluid Dynamics*, Gunzberger MD, Nicolaides RA (eds). Cambridge University Press: Cambridge, 1993; 183–201.

DOI: 10.1002/nag

22. Codina R, Blasco J. A finite element formulation for the Stokes problem allowing equal velocity–pressure interpolation. *Computer Methods in Applied Mechanics and Engineering* 1997; **143**:373–391.
23. Codina R, Vázquez M, Zienkiewicz QC. A fractional step method for compressible flows boundary conditions and incompressible limit. In *Proceedings of the International Conference on Finite Elements in Fluids-New Trends and Applications*, Morandi-Cecchi M, Morgan K, Periaux J, Schrefler BA, Zienkiewicz OC (eds). Venezia, 1995; 409–418.
24. Li XK, Duan QL. Meshfree iterative stabilized Taylor–Galerkin and characteristic-based split (CBS) algorithms for incompressible N–S equations. *Computer Methods in Applied Mechanics and Engineering* 2006; **195**:6125–6145.

DOI: 10.1002/nag